



HAL
open science

Synthesis of Visible Light Excitable Carbon Dot Phosphor-Al₂O₃ Hybrids for Anti-Counterfeiting and Information Encryption

Dong Lu, Ke Lu, Hong-tao Wen, Zhan Wei, Alberto Bianco, Gui-gen Wang,
Hua-yu Zhang

► **To cite this version:**

Dong Lu, Ke Lu, Hong-tao Wen, Zhan Wei, Alberto Bianco, et al.. Synthesis of Visible Light Excitable Carbon Dot Phosphor-Al₂O₃ Hybrids for Anti-Counterfeiting and Information Encryption. *Small*, 2023, Carbon Nanodots: Nanolights Illuminating a Bright Future, 19 (31), pp.2207046. 10.1002/sml.202207046 . hal-04248902

HAL Id: hal-04248902

<https://hal.science/hal-04248902v1>

Submitted on 18 Oct 2023

HAL is a multi-disciplinary open access archive for the deposit and dissemination of scientific research documents, whether they are published or not. The documents may come from teaching and research institutions in France or abroad, or from public or private research centers.

L'archive ouverte pluridisciplinaire **HAL**, est destinée au dépôt et à la diffusion de documents scientifiques de niveau recherche, publiés ou non, émanant des établissements d'enseignement et de recherche français ou étrangers, des laboratoires publics ou privés.

Synthesis of visible light excitable carbon dot phosphor- Al_2O_3 hybrids for anti-counterfeiting and information encryption

Dong Lu, Ke Lu, Hong-Tao Wen, Zhan Wei, Alberto Bianco, Gui-Gen Wang,* Hua-Yu Zhang,**

D. Lu, H.-T. Wen, Z. Wei, G.-G. Wang, H.-Y. Zhang

Shenzhen Key Laboratory for Advanced Materials, School of Materials Science and Engineering,
Harbin Institute of Technology (Shenzhen), Shenzhen 518055, PR China

E-mail: wangguigen@hit.edu.cn; hzyzhang@hit.edu.cn

K. Lu

School of Advanced Materials, Shenzhen Graduate School, Peking University, Shenzhen 518055, PR
China

D. Lu, A. Bianco

CNRS, Immunology, Immunopathology and Therapeutic Chemistry, UPR 3572, University of
Strasbourg, ISIS, 67000 Strasbourg, France

E-mail: a.bianco@ibmc-cnrs.unistra.fr

Keywords: Carbon materials; aluminium hydroxide; calcination; room temperature phosphorescence;
multicolour emissions

ABSTRACT

The preparation of room temperature phosphorescent carbon dots still faces great challenges, especially in the case of carbon dots endowed of visible-light excitable room temperature phosphorescence (RTP). To date, a limited number of substrates have been exploited to prepare room temperature phosphorescent carbon dots, and most of them can emit RTP only in solid state. Here, we report the synthesis of a composite obtained from the calcination of green carbon dots (g-CDs) blended with aluminium hydroxide ($\text{Al}(\text{OH})_3$). The resultant hybrid material $\text{g-CDs@Al}_2\text{O}_3$ exhibits blue fluorescence and green RTP emissions in an *on/off* switch process at 365 nm. Notably, this composite manifests strong resistance to extreme acid and basic conditions up to 30 days of treatment. The dense structure of Al_2O_3 formed by calcination contributes to the phosphorescent emission of g-CDs. Surprisingly, $\text{g-CDs@Al}_2\text{O}_3$ can also emit yellow RTP under irradiation with white light. The multicolour emissions can be employed for anti-counterfeiting and information encryption. Finally, our work provides a universal and straightforward approach to produce room temperature phosphorescent carbon dots for a wide range of applications.

1. Introduction

Materials endowed of room temperature phosphorescence (RTP) can emit this type of light in ambient conditions, rather than at low temperature or in anaerobic environments. Thanks to this unique property, these materials have drawn a lot of attention and have been successfully applied in many fields, such as sensing, optoelectronics, anti-counterfeiting, and information encryption.^[1] The development of RTP materials with multicolour emissive fluorescence (FL) and phosphorescence (Phos) represents a promising approach to ensure information safety during their transmission.^{Erreur ! Source du renvoi introuvable.} Recently, visible-light excitable RTP materials came into the focus of research as they are less harmful to human, they have deeper tissue penetrability, and they are more convenient as encrypting tags.^{Erreur ! Source du renvoi}

introuvable. Traditional RTP materials are usually made of inorganic composites containing rare metals or organic coordination complexes. These substances display often high toxicity, require complex synthesis and purification protocols which are costly, thus limiting their broad applications. Developing superior visible-light excitable and cost-effective room temperature phosphorescence materials is therefore urgent.

Carbon dots (CDs),^{Erreur ! Source du renvoi introuvable.} as zero-dimensional nanomaterials, whose size is below 10 nm, have emerged as a novel carbon form with a wide range of applications, including catalysis,^[11] sensing,^[12, 13] information security,^[4] and bioimaging fields.^{Erreur ! Source du renvoi introuvable.} This is certainly due to their numerous merits, such as remarkable optical performance, high water solubility, low toxicity, high resistance to photobleaching, and versatile chemical modifications.^{Erreur ! Source du renvoi introuvable.} Recently, it has been reported that CD hybrids prepared using organic and inorganic materials, could be useful RTP materials.^{Erreur ! Source du renvoi introuvable.} Up to now, only a few substrates have been successfully applied to prepare RTP CDs, including polyvinyl alcohol,^{Erreur ! Source du renvoi introuvable.} boric acid,^{Erreur ! Source du renvoi introuvable.} and silica gel.^{Erreur ! Source du renvoi introuvable.} In comparison to traditional RTP materials, CDs also own the advantage of using diverse methods and a potentially unlimited choice of raw materials for their synthesis. CDs were demonstrated to generate RTP only under UV light irradiation, while the excitation using visible light remained unexplored, as these materials are rarely visible light excitable.^{Erreur ! Source du renvoi introuvable.} In addition, most of CDs are unable to withstand extreme conditions and are incapable of emitting RTP in aqueous environment. These shortcomings have limited their practical applications. In 2020, Sun *et al.* have developed ultra-long lifetime hydrophilic RTP CDs using rice husk containing silicon as raw materials, to obtain silicon-doped CDs after calcination. The dots showed over 40 s afterglow with a lifetime up to 5.72 s.^{Erreur ! Source du renvoi introuvable.} However, this material did not emit Phos under excitation with visible light. In an alternative approach, the group of Dong reported nitrogen-doped CDs derived from

diethylenetriaminepentaacetic acid, formed by hydrothermal method. These CDs resulted phosphorescent at room temperature after visible light excitation thanks to their inner hydrogen bond skeleton. The hydrogen bonds played a critical role to promote the $n-\pi^*$ transition and boosting the intersystem crossing so that the excitons in the triplet state could trigger the carbon dot phosphorescence. However, these carbon dots did not emit phosphorescence in aqueous solutions and were not resistant to extreme condition.^{Erreur ! Source du renvoi introuvable.} Very recently, RTP emissive carbon dots were reported for applications in multi-patterning, anti-counterfeiting and information encryption.^[27, 28] Alternatively, Wang *et al.* produced RTP CDs by embedding rhodamine B in a B_2O_3 matrix, obtaining a material with an afterglow lasting for over 10 s, which was also successfully applied for information encryption.^{Erreur ! Source du renvoi introuvable.} Nevertheless, boron oxide might generate toxic effects at high doses once released in the environment,^{Erreur ! Source du renvoi introuvable.} and it is easily corroded by strong bases. Besides, this kind of CDs seems not to be phosphorescent at room temperature in water. On the basis of the available data, it is still a great challenge to prepare room temperature phosphorescent CDs emitting phosphorescence under visible light in aqueous solution, and very resistant to harsh conditions.

Inspired by boron containing CD hybrids, we thought to replace the element B with Al, which belong to the same periodic group and has similar electronic configuration. Meanwhile, aluminium oxides possess rigid chemical structure, while Al is one of the most abundant element in our planet, suitable substrate to develop low-cost RTP CDs likely endowed of interesting optoelectronic properties.

In this work, we reported the synthesis of a $g\text{-CDs}@Al_2O_3$ composite, in which aluminium hydroxide acted as rigid matrix to preserve and tune the phosphorescent properties of $g\text{-CDs}$. The $g\text{-CDs}@Al(OH)_3$ precursor of $g\text{-CDs}@Al_2O_3$ showed azure photoluminescence, but no phosphorescence before undergoing high-temperature calcination. Increasing the temperature during the calcination process, aluminium hydroxide underwent a dehydration process and its

structure changed from $\text{Al}(\text{OH})_3$ to AlOOH and Al_2O_3 .^{Erreur ! Source du renvoi introuvable.} As a consequence, the matrix of the aluminium compound became more compact and enhanced the stability of the triplet state of g-CDs to emit Phos. It is worth noting that this calcinated Phos CDs can emit yellow Phos under white light irradiation, while releasing green Phos under 365 nm UV lamp illumination. Remarkably, these dots also emit phosphorescence in aqueous media and possess long-lasting resilience to harsh acid and base conditions. To prove the wide versatility of our approach to generate RTP carbon dots, we also employed various organic molecules, such as anthrurufin and tartaric acid, to produce additional CDs and embed them into $\text{Al}(\text{OH})_3$. After calcination at high temperature ($T \geq 500 \text{ }^\circ\text{C}$), all composites demonstrate to possess green and yellow RTP. Therefore, different phosphorescent carbon dots were obtained by a general and simple method, leading to a material which could be used for information encryption and anti-counterfeiting.

2. Results and discussion

The synthetic process to obtain g-CDs is illustrated in Figure 1. Briefly, 2,4-diaminobenzenesulfonic acid and sulfuric acid were dissolved in pure ethanol and heated at 180°C in an autoclave for 6 h, leading to the formation of the desired g-CDs. Following their purification, the structure, the chemical composition and the electronic properties of the dots were assessed using complementary spectroscopic and microscopic techniques. The size and the crystal lattice of g-CDs was evidenced by high-resolution TEM (HR-TEM), measuring a spacing between the atoms of 0.26 nm, similar to the value reported in the literature (Figure 2a, 2b and S1).^{Erreur ! Source du renvoi introuvable.} The average size of g-CDs is centred at 4.4 nm (see inset in Figure S1a). The Raman spectrum of g-CDs shows the presence of the disordered (D) and graphitic (G) bands situated at 1361 cm^{-1} and 1578 cm^{-1} , respectively (Figure S2).^{Erreur ! Source du renvoi introuvable.} To further characterize g-CDs, $^1\text{H-NMR}$ (Figure S3a) and $^{13}\text{C-NMR}$ analysis (Figure S3b) of the starting molecules and the final dots were carried

out. **Erreur ! Source du renvoi introuvable.** No residual precursor molecules were observed in the purified g-CDs (Figures S4-7). The surface chemistry of g-CDs was then studied by FT-IR and XPS. The FT-IR spectrum of g-CDs shows the presence of the functional groups corresponding to the stretching of N-H/O-H (3455 cm^{-1}), C=C (1641 cm^{-1}), C-N (1400 cm^{-1}), and SO₃ (1108 cm^{-1}), respectively (Figure S8). The XPS survey spectrum of g-CDs displays the presence of four main elements (Figure 2g and Figure S9a). Their percentages correspond to 57.3% of carbon, 13.9% of nitrogen, 23.2% of oxygen, and 5.6% of sulfur (Figure S9b). The high-resolution C1s spectrum shows the typical peak associated to C=C/C-C at 284.7 eV, C-O peak located at 286.1 eV and C-N/C-S peak at 285.2 eV (Figure S9c). The high-resolution N1s spectrum is characterized by the combination of amino (401.5 eV), pyrrolic (399.4 eV), pyridinic (398.7 eV), and quaternary graphitic (400.2 eV) nitrogen bonds (Figure S9d). **Erreur ! Source du renvoi introuvable.** Due to the use of a high amount of H₂SO₄ during the reaction, the thermal treatment causes an extensive oxidation of the material, leading to the formation of surface oxygenated functions (Figure S9e). Since the starting 2,4-diaminobenzenesulfonic acid contains a sulfur atom, this reagent contributed, together with sulfuric acid, to the insertion of sulfur moieties into g-CDs. The high-resolution S2p spectrum is ascribed to the presence of C-SO_x groups corresponding to three peaks at 167.6 eV, 168.3 eV, and 169.2 eV (Figure S9f). **Erreur ! Source du renvoi introuvable.**

Following the chemical and structural characterization, the optical properties of g-CDs were analyzed. The excitation and emission spectra of g-CDs are displayed in Figure S10a. The maximum values of excitation and emission correspond to 412 and 534 nm, respectively. The g-CDs have wide and strong absorption peaks in the visible range (350-550 nm) and green FL under 365 nm excitation (blue curve in Figure S10a). we also found that g-CDs have a quasi-identical emissive wavelength with the excitation wavelength changing from 360 to 540 nm (Figure S10b), with a constant emission peak located at 534 nm. As shown in the up-conversion emission spectra of g-CDs (Figure S10c) using excitation wavelengths in the near-

infrared range (750-900 nm), the emission peak is still located at 534 nm, evidencing the maximum up-conversion excitation wavelength centered at 850 nm (green curve in Figure S10c). This result proves that the g-CDs possess up-conversion emission properties with prospective applications in bioimaging and photodetection.^{Erreur ! Source du renvoi introuvable.} As-obtained g-CDs were then tested for their stability at extreme pH conditions (Figure S11a). Only in highly alkaline conditions (pH = 13), the fluorescence intensity of carbon dots decreases significantly although the emission peak remains centered nearby 534 nm. The analysis of g-CDs dispersed at different concentrations in water reveals significant differences. The emission wavelength augmented from 513 nm to 555 nm with increasing concentrations, shifting the photoluminescence from green to yellow. At the concentration of 0.10 mg/mL, the green carbon dots show the strongest FL intensity (Figure S11b).

After complete characterization of g-CDs, we decided to mix them with Al(OH)₃ and to dry them to obtain a blue fluorescent powder corresponding to g-CDs@Al(OH)₃ (Figure 1). Following a high temperature calcination (≥ 500 °C), the material was finally transformed into g-CDs@Al₂O₃, unexpectedly emitting phosphorescence after UV light excitation (Figure 3a).

The HR-TEM images of the starting g-CDs@Al(OH)₃, evidenced a layered structure of hundreds of nanometers in lateral size (Figure 2c).^{Erreur ! Source du renvoi introuvable.} The magnifications of the HR-TEM micrographs allow to observe the crystalline g-CDs embedded into the aluminium hydroxide matrix (Figure 2d). The HR-TEM images recorded post-calcination of g-CDs@Al(OH)₃ display an aluminium compound with a more compact structure (Figure 2e). Similarly to starting g-CDs@Al(OH)₃, we could observe the lattice fringes of carbon dots on the surface of g-CDs@Al₂O₃ (Figure 2f). The spectra of XPS surveys of g-CDs, g-CDs@Al(OH)₃ and g-CDs@Al₂O₃ are compared in Figure 2g. The ratios of the elements before and after calcination are reported in Table S1. Al and O clearly account for the largest contribution originating from Al(OH)₃. C, N, and S belong instead to g-CDs,

and the content of these elements are decreased during the calcination. The proportion of carbon is reduced from 30.0% to 17.1% after 500 °C thermal treatment. The low content N and S is vanished after this process, probably because nitrogen and sulfur atoms are below the detection limit (Figure S12).

As a small amount of g-CDs incorporated into Al(OH)₃ generated a powder emitting a bright blue fluorescence likely originating from carbon dots, while phosphorescence was absent, we decided to study more in depth this phenomenon. We first verified that Al(OH)₃ alone had no fluorescence emission before and after calcination (Figure S13). After calcination above 500 °C, the powder of the hybrid g-CDs@Al₂O₃ could emit green RTP (Figure 3a). During the heating process, the structure of Al(OH)₃ is transformed into a dense Al₂O₃ lattice, leading the embedded g-CDs to emit green phosphorescence. To understand the luminescent and phosphorescent mechanisms, we performed the XRD diffraction pattern analysis of g-CDs@Al(OH)₃ composite at increasing calcination temperatures to disclose the phase changes (Figure 2h and 2i). At a temperature below 200 °C, Al(OH)₃ maintain its original chemical structure, while it starts to lose H₂O molecules as the temperature surpassed 200 °C, converting the hydroxide into AlOOH intermediates.^{Erreur ! Source du renvoi introuvable.} As the temperature ramped up, the dehydration of aluminium composites is continued and AlOOH intermediates became Al₂O₃ when the sample was heated at 500 °C. The XRD data allowed to verify the structural transformation of the aluminium composite as previously reported.^{Erreur ! Source du renvoi introuvable.}

Since the calcination process of Al(OH)₃ endowed g-CDs with RTP, we further studied the photophysical properties of g-CDs@Al₂O₃ (Figure 3b-e). Figure 3b shows the FL and Phos emission spectra under UV light excitation at 360 nm, evidencing the two maximum emission peaks at 438 nm and 510 nm, respectively. The luminescence and the green afterglow of g-CDs@Al₂O₃ last for 5 s (Figure 3a, 3c and Video S1). Surprisingly, g-CDs@Al₂O₃ presented instead a yellow afterglow after switching off the irradiation using a white light (Figure 3c

and Video S1). The lifetime of phosphorescence emission of g-CDs@Al₂O₃ was also recorded (Figure S14) and compared to that of g-CDs alone (Figure S15). The curves of the two materials followed double exponential decay. The two lifetime values for g-CDs corresponded to $\tau_1 = 5.0$ ns and $\tau_2 = 8.37$ ns, with an average τ_{ave} of 5.96 ns.^[23] The phosphorescent lifetime calculation for g-CDs@Al₂O₃ afforded a $\tau_1 = 71.49$ μ s and a $\tau_2 = 875.57$ μ s, with an average lifetime τ_{ave} corresponding to 736.57 μ s. Based on these data, we propose a possible mechanism for the fluorescence and the phosphorescence properties of g-CDs@Al₂O₃ (Figure 3c). Under UV irradiation, the ground state (S₀) of carbon dots is able to absorb the excitons (high energy photons) reaching the excited state (¹S₁) (magenta zone in Figure 3c). The excited state (¹S₁) is unstable and can return to S₀ emitting fluorescence (blue zone in Figure 3c). But owing to the confinement exerted by Al₂O₃, the energy of the carbon dots in ¹S₁ is transferred to the triplet state (¹T₁) and g-CDs can maintain a long-lasting ¹T₁ emitting phosphorescence (green zone in Figure 3c). The energy gap between ¹S₁ and ¹T₁ (E_{ST}) is 0.40 eV. The energy gap is close enough that the energy can be easily transferred from the single (¹S₁) excited state to the triple (¹T₁) excited state. In the case of white light excitation, the excitons in the single (¹S₁) excited state transfer their energy to the triple (¹T₁) excited state emitting yellow phosphorescence when the system returns to the ground state.^[25]

After elucidating the fluorescence and phosphorescence characteristics of g-CDs, the illumination values of the different g-CDs in liquid and solid state were plotted using the CIE (Commission International de l'Eclairage) coordinate diagram (Figure S16). Initially, FL coordinates of aqueous g-CDs are located in the green region (no. 1). Once blended with Al(OH)₃, the carbon dots are changed to blue FL (no. 2). Finally, the calcination of g-CDs@Al(OH)₃ affording g-CDs@Al₂O₃ turns FL into green RTP (no. 3). The variety of colour changes offers considerable potential applications in emergency conditions, like for examples in chemical factories undergoing fire accidents where the visual alarm tools need to resist to corrosive gas emissions.

In this context, as we verified the behavior of g-CDs in a wide range of pH (Figure S11), we also tested the stability and emission properties of g-CDs@Al₂O₃ in extremely harsh conditions. FL and green RTP performances of g-CDs@Al₂O₃ under extreme acidic (5 M H₂SO₄) and alkaline (5 M KOH solution) conditions are only slightly affected (Figure 3d and 3e). The fluorescence intensity of g-CDs@Al₂O₃ in alkaline solution is nearly unchanged after 30 days (red line in Figure 3d), and the same composite also demonstrates strong resistance to acid solution (green line in Figure 3d). Similarly, g-CDs@Al₂O₃ preserves excellent RTP performances after 30 days in both acidic and basic conditions (Figure 3e). Unlike the other types of solid-state Phos carbon dot composites (e.g., made of H₃BO₃, KAl(SO₄)₂, PVA, or urea as substrates), our composite does not dissolve or lose phosphorescence in extreme liquid conditions. Video S2 displays the green RTP emission of g-CDs@Al₂O₃ in deionized water, showing that the aqueous afterglow persisted for approximately 2 s.

To explore further the phosphorescent properties of g-CDs@Al₂O₃ powder, we first simply blended this hybrid with RhB at room temperature. Unexpectedly, we obtained a material able to emit red phosphorescence which is visible by naked eyes after switching off UV light (Figure 4a). According to Förster resonance energy transfer (FRET) theory, the emission spectra of g-CDs and RhB are overlapped, fulfilling the conditions of FRET. The g-CDs play the role of donor and RhB that of acceptor. Therefore, the energy transferred from the dots to RhB triggers the emission of rhodamine red phosphorescence.^[37] Then, following the first synthetic strategy to prepare Phos carbon dot composites, five different precursors, including 8-hydroxypyrene-1,3,6-trisulfonic acid (**I**), 1,5-dihydroxyanthraquinone (**II**), DL-tartaric acid (**III**), perylene-3,4,9,10-tetracarboxylic dianhydride (**IV**), and 5-amino-1-naphthalenesulfonic acid (**V**) were used to replace 2,4-diaminobenzenesulfonic acid in the synthesis of a library of carbon dots (see Supporting Information for Experimental details). Five carbon dots with fluorescence and phosphorescence emission were obtained after applying a high temperature

calcination process (Figure S17). The maximum emission FL peaks of four of these composites (namely **I/II/III/V**) are located in the blue region (437-450 nm), whereas their Phos peaks appear in the green region (505-536 nm). FL and Phos emission bands of composite **IV** are instead centred at 473 nm (cyan) and 553 nm (yellowish green), respectively. Video S3 shows the true digital record of FL and yellow/yellowish green RTP emission of composite **IV** at different excitation wavelengths. The real-time fluorescent and phosphorescent photos of all five composites under UV/white light irradiation are displayed in Figure S18. The first yellow dashed column allows to observe by naked eyes the phosphorescence emission with different intensities when white light was turned off. Only the composite **IV** reveals a subtle yellow RTP. The other columns show FL and RTP of the five composites **I/II/III/IV/V** when the 365 nm lamp was switched *on/off*. The afterglow lasted for 2 to 5 s (Figure S18). The phosphorescence quantum yields (QYs) of g-CDs@Al₂O₃ and the composites I-V were finally measured. The values of the QYs of g-CDs@Al₂O₃ and the five composites are 42.6%, 36.9%, 21.2%, 17.2%, 10.2% and 6.6%, respectively. We can notice that the QY of g-CDs@Al₂O₃ is the highest, proving that the choice of the precursors for the synthesis of the dots and the post-calcination process are critical in obtaining carbon dots with high phosphorescence QY. Indeed, it has been reported that the quantum yield can be affected by the level of dehydration increasing the temperature of carbonization or by the doping with heteroatoms.^[38, 39]

With the different g-CD composites in hands, we decided to explore their phosphorescent properties for potential applications in information encryption. For this purpose, we combined three phosphors and a control hybrid to shape and illuminate the **HIT** pattern (HIT representing the initial letters of Harbin Institute of Technology). Powder 1 consisting on RhB mixed with Al(OH)₃ without calcination could only emit red FL without Phos emission. After turning off UV light irradiation, powder 2 consisting of RhB mixed with g-CDs@Al₂O₃ emitted weak and transitory red Phos. Powder 3 corresponding to g-CDs@Al₂O₃ and powder

4 consisting on composite **IV** radiated instead distinct green light lasting for few seconds after turning off the UV lamp (Figure 4a). When **HIT** was irradiated with white light only powder 4 emitted yellow RTP when the lamp was turned off (Figure 4a).^{Erreur ! Source du renvoi introuvable.} Consequently, we could exploit the luminescent characteristics of the four powders to achieve information encryption by combining the responses of *on/off* signals of UV and white lights, as illustrated by the schematic diagram in Figure 4b. Through this method, we could transmit specific messages relying on a safe multi-channel approach. For instance, we can mix together channels 1 to 4 to form a password. If the password is the number 243, the channels will decode 2 by IIT, 4 by T, and 3 by IT, respectively. The three number of the password would correspond to the message **IITIT**. If we change the password to 321, we obtain a new information corresponding to the message **ITITHIT**. We could also use these powder to form a cartoon profile or other characters (similar to H of **HIT**). The *on/off* mode will transmit different information, e.g., one true and the other false, hence, reaching the goal of information encryption. Finally, Phos powder 2 were dispersed in a small amount of water to dip the thumb and press a fingerprint on a paper. When UV excitation was *off*, we can discriminate the clear fingerprint patterns evidenced by the purple dashed line (Figure 4c). The afterglow of the fingerprint can last for over 2 s, and the texture could be clearly distinguished by naked eyes even 1 s after switching off the UV light. These results highlight how our g-CD-based phosphorescent composites can be used in fingerprint recognition and anti-counterfeiting exploiting RTP, particularly using white light excitation.

3. Conclusion

In this study, a new approach was proposed to obtain green fluorescent carbon dots, subsequently blended with aluminium hydroxide to form room temperature phosphorescent carbon dot composites. The thermal treatment of g-CDs@Al(OH)₃ transforms the hybrid into

a more structurally compact Al_2O_3 , leading to a strong confinement of the vibrations of the chemical bonds in g-CDs. Consequently, the triplet state of g-CDs become more stable and can emit green and yellow RTP using UV or white light excitation wavelength, respectively. The afterglow of g-CDs@ Al_2O_3 lasted for over 5 s. Our methodology was then expanded to the synthesis of other composites using different raw materials blended to $\text{Al}(\text{OH})_3$ and heated at high temperatures generating composites with yellow RTP turning off white light illumination, and with green RTP when 365 nm excitation was instead switched off. CDs@ Al_2O_3 composites own also considerable capability to withstand the interference of harsh conditions, expanding further their applications. Overall, this work covers a general and practical method to prepare multicolour RTP carbon dots excitable by visible light.

4. Experimental Section

4.1. Materials

2,4-Diaminobenzenesulfonic acid, 5-amino-1-naphthalenesulfonic acid, DL-tartaric acid, 8-hydroxypyrene-1,3,6-trisulfonic acid, 1,5-dihydroxyanthraquinone, perylene-3,4,9,10-tetracarboxylic dianhydride Rhodamine B (RhB), aluminium hydroxide, and ethanol were purchased from Aladdin Industrial Co. Ltd (Shanghai, China). Ammonium hydroxide was obtained from Sinopharm Chemical Reagent Co., Ltd. (Shanghai, China). All reagents were used without further purification.

4.2. Characterizations

The fluorescence spectra of g-CDs dispersed in deionized water were obtained from Thermo Fisher Lumina. The measurement of the phosphorescence spectra and fluorescence spectra of solid state g-CD phosphors were performed on a F-7000 spectrophotometer (Hitachi, Japan). The lifetime of CD phosphors was obtained by a FLS980 spectrophotometer (Edinburgh Instrument, UK), equipped with a microsecond flash-lamp (mF900). All phosphorescence measurements were performed using the excitation wavelength at 360 nm. The UV-Vis

absorption spectra were collected by Thermo Fisher Evolution 300 spectrophotometer. Fourier transform infrared (FT-IR) absorption spectra were acquired by Thermo Nicolet IS50. Raman spectra were measured using a Renishaw Quantor. X-ray powder diffraction (XRD) patterns were recorded on Panalytical Aries X-ray diffractometer with Cu K α radiation ($\lambda = 1.54056 \text{ \AA}$). High-resolution transmission electron microscopy (HR-TEM) images were acquired using a JEM-3200FS (JEOL). X-ray photoelectron spectroscopy (XPS) analysis and elemental content were measured using a ESCALAB 250Xi. AVANCE-III (Bruker, 400 MHz) was employed to obtain the $^1\text{H-NMR}$ and $^{13}\text{C-NMR}$ spectra. All optical images and videos were recorded by an Honor 20 lite smart phone (Honor, China). The phosphorescence quantum yields (Phos QY) were performed using PICOQuant FT-300 (PiccoQuant, Germany) using an integrating sphere.

4.3. Synthesis of g-CDs

Green carbon dots were synthesized following a solvothermal treatment. 2,4-Diaminobenzenesulfonic acid (0.5 g) was dispersed in 22 mL of ethanol and 3 mL of 5 M sulfuric acid. The reagents underwent ultrasonication (JP-040, Skymen Co., Ltd., China) for 10 min before transfer into an autoclave and heating for 6 h at 180 °C. The solution was then filtered through a 0.22 μm membrane three times to remove large particles. The filtered solution was purified via silica column chromatography using ethanol and acetic ether as the eluents, and dried *in vacuo* to obtain pure g-CD powder. The powder was dissolved in deionized water at concentration of 0.05, 0.10, 1.0, 2.0, and 5.0 mg/mL of g-CDs for next steps.

4.4 Synthesis of g-CDs@Al(OH) $_3$, g-CDs@Al $_2$ O $_3$, RhB@Al(OH) $_3$ and RhB/g-CDs@Al $_2$ O $_3$

g-CDs@Al(OH) $_3$ hybrid was synthesis by mixing 0.1 mL of 0.1 mg/mL of g-CDs solution with 2.0 g of Al(OH) $_3$ powder is 5 mL of deionized water. This mixture was placed in heating oven (Youyi Instrument Co., Ltd, China) at T = 100 °C to dry affording g-CDs@Al(OH) $_3$ powder. g-CDs@Al $_2$ O $_3$ was synthesized through calcination for 2 h, setting the temperatures

at 200, 300, 400, 500, 600 and 650 °C, respectively. During this process, g-CDs@Al(OH)₃ hybrid loose water molecules to become g-CDs@Al₂O₃ composite at the temperature above 500 °C. Fifty μg of RhB and 2 g of Al(OH)₃ powder were blended and dispersed into deionized water (5 mL) to form RhB@Al(OH)₃, then the mixture was dried under 100 °C. Fifty μg of RhB and 2 g of g-CDs@Al₂O₃ powder were blended and dispersed into deionized water (5 mL) to form RhB/g-CDs@Al₂O₃. The dispersion was subsequently freeze dried to obtain RhB/g-CDs@Al₂O₃ powder.

4. 5. Stability at different pH

g-CDs@Al₂O₃ powder (100 mg) was dispersed using ultrasonic treatment into 5 M of H₂SO₄ (2 mL) and 5 M KOH solutions (2 mL), respectively. The fluorescence and phosphorescence spectra of these solutions were acquired after 1 day and after 30 days to compare the resistance to harsh condition.

Acknowledgements

This work was funded by the National Natural Science Foundation of China (No. 52072094 and No. 52272036), and financial support from the program of China Scholarships Council. The work was supported by Fund of National Key Laboratory of Science and Technology on Advanced Composites in Special Environments (Grant No. 6142905192507), Shenzhen Science and Technology Plan Supported Project (Grant No. GXWD20201230155427003-20200821232246001, JCYJ20170413105844696).

References

- [1] X. Chen, W. Dai, X. Wu, H. Su, C. Chao, Y. Lei, J. Shi, B. Tong, Z. Cai, Y. Dong, *Chem. Eng. J.* **2021**, *426*, 131607.
- [2] X. Yang, D. Yan, *Chem. Sci.* **2016**, *7*, 4519.
- [3] D. Lou, Y. Sun, J. Li, Y. Zheng, Z. Zhou, J. Yang, C. Pan, Z. Zheng, X. Chen, W. Liu, *Angew. Chem. Int. Ed.* **2021**, *61*, e202117066.
- [4] Y. Han, M. Li, J. Lai, W. Li, Y. Liu, L. Yin, L. Yang, X. Xue, R. Vajtai, P. M. Ajayan, L. Wang, *ACS Sustain. Chem. Eng.* **2019**, *7*, 19918.
- [5] T. U. Connell, P. S. Donnelly, *Coord. Chem. Rev.* **2018**, *375*, 267.
- [6] X. Xu, R. Ray, Y. Gu, H. J. Ploehn, L. Gearheart, K. Raker, W. A. Scrivens, *J. Am. Chem. Soc.* **2004**, *126*, 12736.
- [7] V. Meunier, C. Ania, A. Bianco, Y. Chen, G. B. Choi, Y. A. Kim, N. Koratkar, C. Liu, J. M. D. Tascon, M. Terrones, *Carbon* **2020**, *195*, 272.
- [8] D. Lu, Y. Tang, J. Gao, Q. Wang, *J. Mater. Chem. C* **2018**, *6*, 13013.
- [9] X. Li, Z. Zhou, C. C. Zhang, Y. Zheng, J. Gao, Q. Wang, *Inorg. Chem.* **2018**, *57*, 8866.
- [10] D. Lu, Y. Tang, J. Gao, Y. Chen, Q. Wang, *Dyes Pigm.* **2019**, *165*, 287.
- [11] C.-L. Shen, Q. Lou, K.-K. Liu, L. Dong, C.-X. Shan, *Nano Today* **2020**, *35*, 100954.
- [12] X. Tang, H. Yu, B. Bui, L. Wang, C. Xing, S. Wang, M. Chen, Z. Hu, W. Chen, *Bioact. Mater.* **2021**, *6*, 1541.
- [13] Y. Xu, H. Yu, L. Chudal, N. K. Pandey, E. H. Amador, B. Bui, L. Wang, X. Ma, S. Deng, X. Zhu, S. Wang, W. Chen, *Mater. Today Phys.* **2021**, *17*, 100328.
- [14] J. Gu, F. Zhang, Z. Zheng, X. Li, R. Deng, Z. Zhou, L. Ma, W. Liu, Q. Wang, *Chin. Chem. Lett.* **2021**, *32*, 87.
- [15] X. Li, M. Li, Y. Chen, G. Qiao, Q. Liu, Z. Zhou, W. Liu, Q. Wang, *Chem. Eng. J.* **2021**, *415*, 128975.
- [16] H.-J. Yu, Q. Zhou, X. Dai, F.-F. Shen, Y.-M. Zhang, X. Xu, Y. Liu, *J. Am. Chem. Soc.* **2021**, *143*, 13887.
- [17] W.-M. He, Z. Zhou, S. Li, Z. Zhou, L.-F. Ma, S.-Q. Zang, *Angew. Chem. Int. Ed.* **2021**, *60*, 8505.
- [18] D. Li, D. Wang, X. Zhao, W. Xi, A. Zebibula, N. Alifu, J.-F. Chen, J. Qian, *Mater. Chem. Front.* **2018**, *2*, 1343.
- [19] J. Gu, X. Li, Z. Zhou, W. Liu, K. Li, J. Gao, Y. Zhao, Q. Wang, *Nanoscale* **2019**, *11*, 13058.
- [20] Y. J. Chung, J. Kim, C. B. Park, *ACS Nano* **2020**, *14*, 6, 6470.
- [21] J. Liu, B. Yang, *ACS Cent. Sci.* **2020**, *6*, 12, 2179.
- [22] J. Jia, W. Lu, Y. Gao, L. Li, C. Dong, S. Shuang, *Talanta* **2021**, *231*, 122350.
- [23] Q. Feng, Z. Xie, M. Zheng, *Chem. Eng. J.* **2021**, *420*, 127647.
- [24] Y. C. Liang, S. S. Gou, K. K. Liu, W. J. Wu, C. X. Shan, *Nano Today* **2020**, *34*, 100900.
- [25] Y. Gao, H. Zhang, S. Shuang, C. Dong, *Adv. Opt. Mater.* **2020**, *8*, 1901557.
- [26] Y. Sun, S. Liu, L. Sun, S. Wu, G. Hu, X. Pang, A. T. Smith, C. Hu, S. Zeng, W. Wang, Y. Liu, M. Zheng, *Nat. Commun.* **2020**, *11*, 5591.
- [27] H.-Y. Wang, L. Zhou, H.-M. Yu, X.-D. Tang, C. Xing, G. Nie, H. Akafzade, S.-Y. Wang, W. Chen, *Adv. Optical Mater.* **2022**, *10*, 2200678.
- [28] D. Gao, P. Wang, F. Gao, W. Nguyen, W. Chen, *Nanomaterials* **2022**, *12*, 2029.
- [29] Z. Xu, X. Sun, P. Ma, Y. Chen, W. Pan, J. Wang, *J. Mater. Chem. C* **2020**, *8*, 4557.
- [30] O. P. Ferreira, S. G. Moraes, N. Durán, L. Cornejo, O. L. Alves, *Chemosphere* **2006**, *62*, 80.
- [31] G. Castruita, Y. A. Perera-Mercado, E. M. Saucedo-Salazar, *J. Inorg. Organomet. Polym. Mater.* **2013**, *23*, 1145.
- [32] Q. H. Pho, L. Lin, N. N. Tran, T. T. Tran, A. H. Nguyen, D. Losic, E. V. Rebrov, V. Hessel, *Carbon* **2022**, *198*, 22.
- [33] P. Yang, Z. Zhu, W. Chen, M. Luo, W. Zhang, T. Zhang, M. Chen, X. Zhou, *J. Lumin.*

- 2020**, 227, 117489.
- [34] F. Arcudi, L. Đorđević, M. Prato, *Angew. Chem. Int. Ed.* **2016**, 55, 2107.
- [35] R. Arrigo, M. Hävecker, S. Wrabetz, R. Blume, M. Lerch, J. McGregor, E. P. J. Parrott, J. A. Zeitler, L. F. Gladden, A. Knop-Gericke, R. Schlögl, D. S. Su, *J. Am. Chem. Soc.* **2010**, 132, 9616.
- [36] D. Kim, J. H. Jung, J. Ihm, *Nanomaterials* **2018**, 8, 375.
- [37] Y.-C. Liang, Q. Cao, K.-K. Liu, X.-Y. Peng, L.-Z. Sui, S.-P. Wang, S.-Y. Song, X.-Y. Wu, W.-B. Zhao, Y. Deng, Q. Lou, L. Dong, C.-X. Shan, *ACS Nano* **2021**, 15, 16242.
- [38] Z. Yi, X. Li, H. Zhang, X. Ji, W. Sun, Y. Yu, Y. Liu, J. Huang, Z. Sarshar, M. Sain, *Talanta* **2021**, 222, 121663.
- [39] S. Wang, H. Niu, S. Hea, Y. Cai, *RSC Adv.* **2016**, 6, 107717.
- [40] J. Tan, Q. Li, S. Meng, Y. Li, J. Yang, Y. Ye, Z. Tang, S. Qu, X. Ren, *Adv. Mater.* **2021**, 33, 2006781.

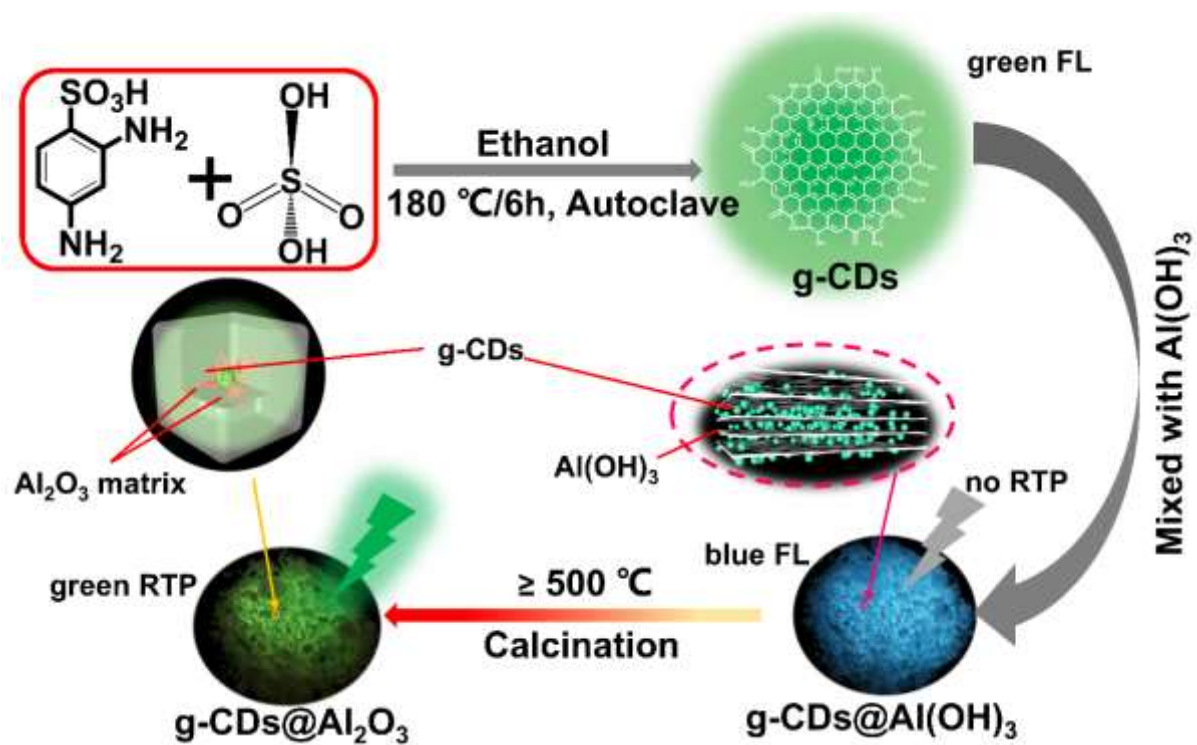


Figure 1 Flow chart illustrating the synthesis of g-CDs@Al(OH)₃ and g-CDs@Al₂O₃ composites.

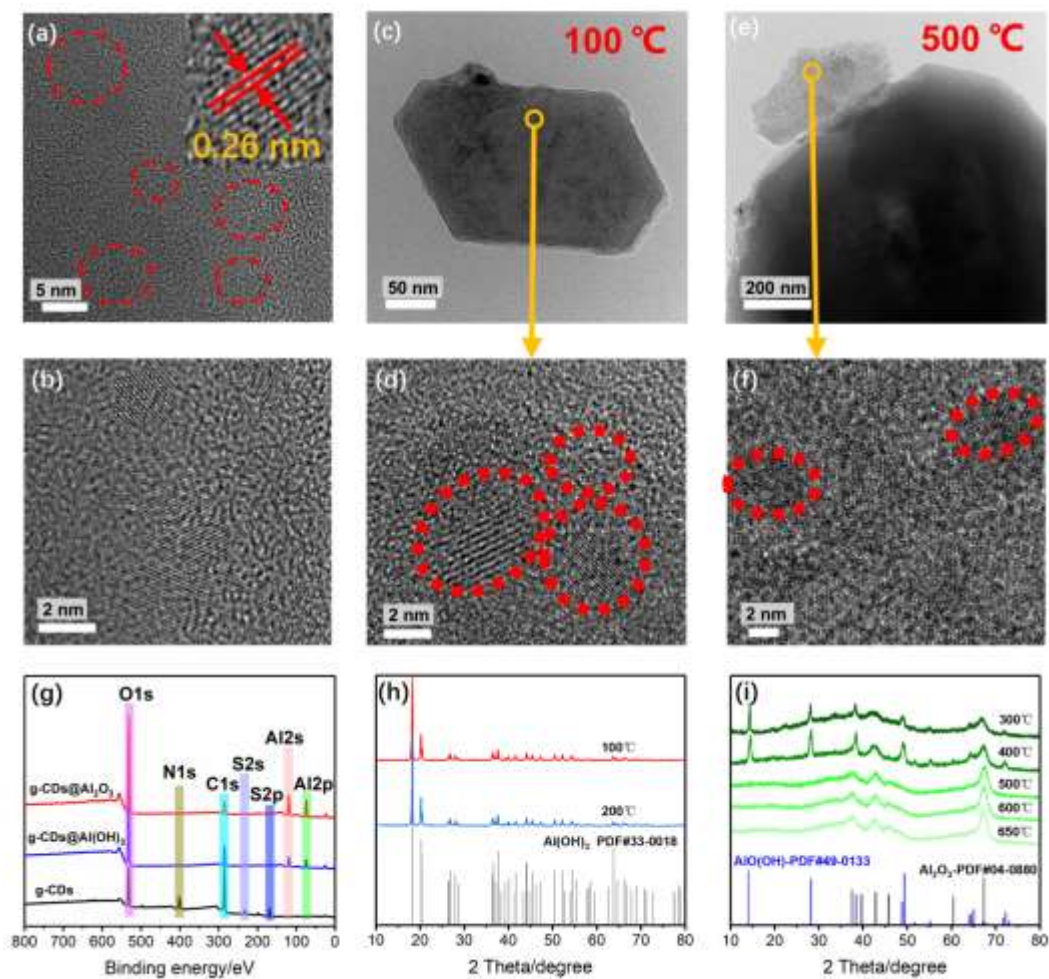


Figure 2 a) HR-TEM image of g-CDs (Inset shows the crystal lattice of g-CDs). b) Magnification of image a). c) HR-TEM image of g-CDs@Al(OH)₃ before calcination. d) Magnification of image c). e) HR-TEM image of g-CDs@Al(OH)₃ after calcination (namely g-CDs@Al₂O₃). f) Magnification of image e). g) XPS survey spectra of g-CDs and g-CDs@Al(OH)₃ and g-CDs@Al₂O₃. h and i) X-Ray diffraction patterns of g-CDs@Al(OH)₃ at different incineration temperatures (100-650 °C).

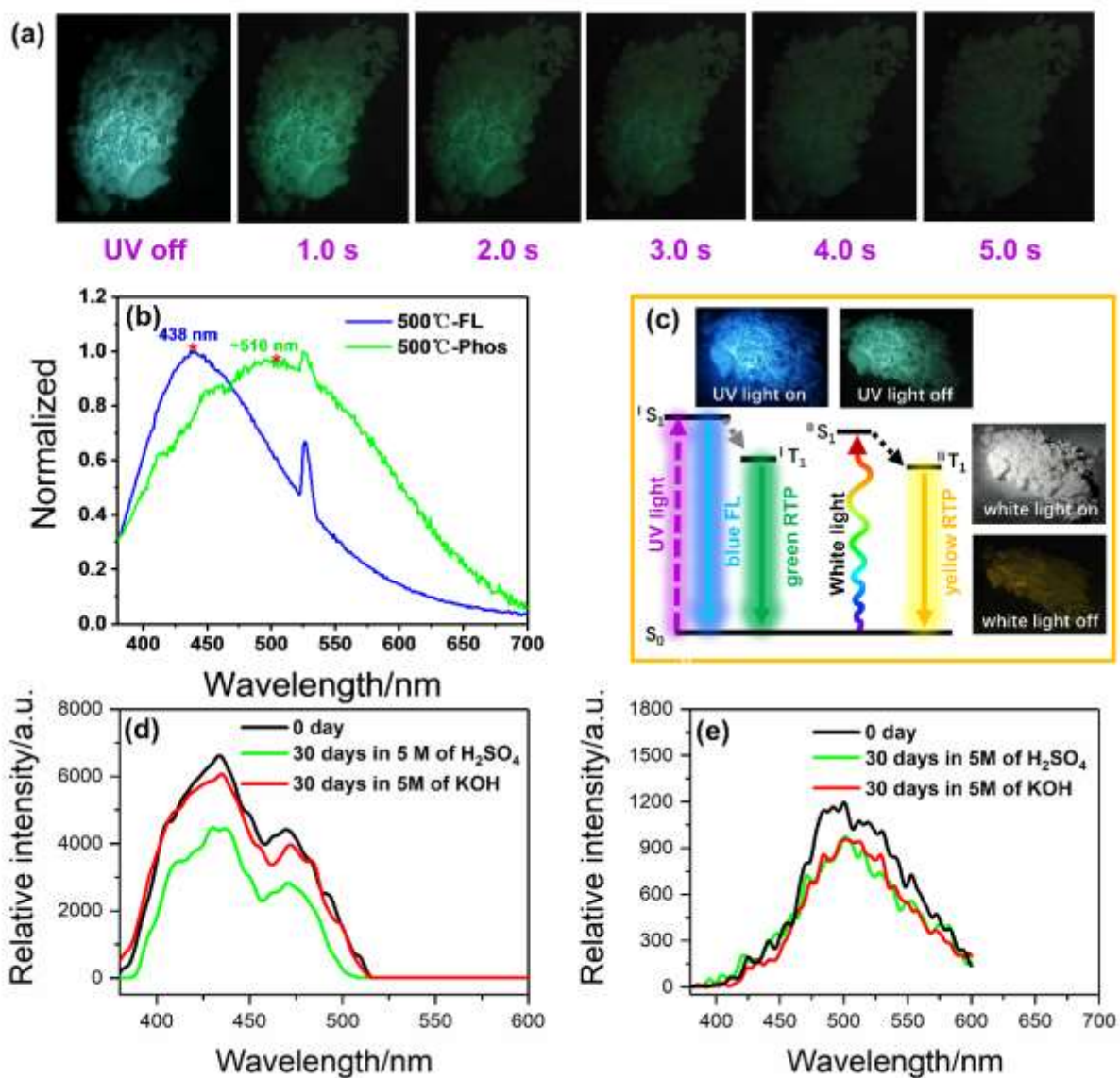


Figure 3 a) Phosphorescence images when 365 nm excitation was *off*, the afterglow lasted for over 5 s. b) The normalized FL and Phos emission spectra of g-CDs@Al₂O₃ ($\lambda_{\text{ex}} = 360$ nm). c) The mechanism of blue FL and green/yellow RTP emission, the insets are the photographs of g-CDs@Al₂O₃ under UV/white light are *on/off*. d) Fluorescence spectra of g-CDs@Al₂O₃ in 5 M of KOH or H₂SO₄ for 30 days ($\lambda_{\text{ex}} = 365$ nm and excitation slit is 1 nm). e) Phosphorescence spectra of g-CDs@Al₂O₃ in 5 M of KOH or H₂SO₄ for 30 days ($\lambda_{\text{ex}} = 365$ nm and excitation slit is 5 nm).

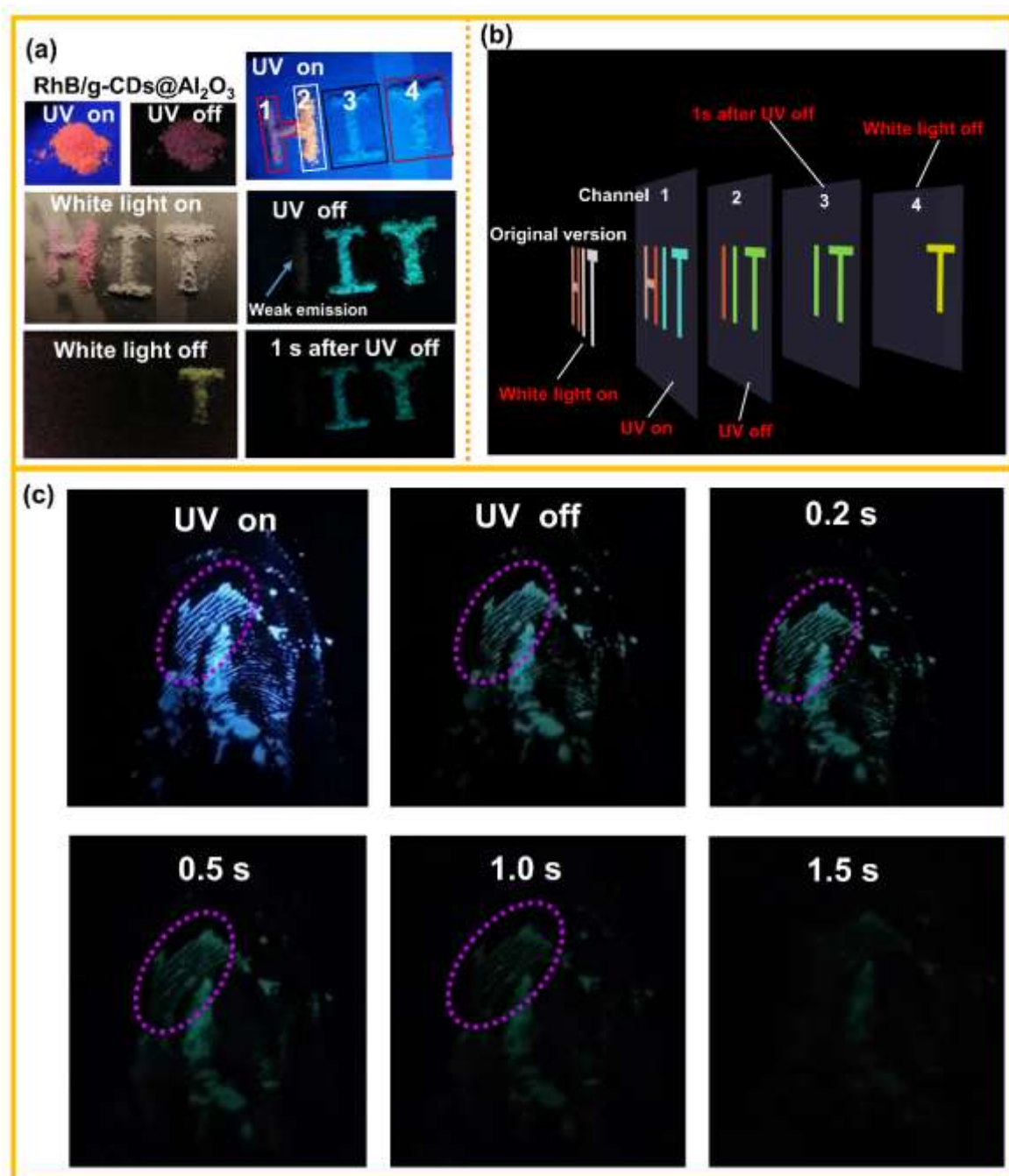


Figure 4 a) Photographs of RhB/g-CDs@Al₂O₃ powder under *on/off* UV light, and four irradiated powders designing **HIT** pattern irradiated by UV and white light (powder 1: RhB mixed with Al(OH)₃ without calcination; powder 2: RhB mixed with g-CDs@Al₂O₃; powder 3: g-CDs@Al₂O₃; powder 4: composite **IV**). b) Schematic diagram of multi-channel emissions employed in information encryption applications. c) Real-time images of a fingerprint made of g-CDs@Al₂O₃ powders.